Journal of Inflammation Research

Dovepress
Taylor & Francis Group

Open Access Full Text Article

ORIGINAL RESEARCH

Revealing the Potential of Solamargine for Anti Metastasis and Angiogenesis Inhibition in Nasopharyngeal Carcinoma

Xiaojuan Tang[1,2], Changju Ma[2], Yuan Ren[1], Yuan Lv[1], Yongheng He[3], Ling Han[2], Jingjing Wu[2]

[1]Central Laboratory, Affiliated Hospital of Hunan Academy of Traditional Chinese Medicine, Changsha, 410006, People's Republic of China; [2]The Second Affiliated Hospital of Guangzhou University of Chinese Medicine, Guangzhou, 510120, People's Republic of China; [3]Department of Anorectal Surgery, Affiliated Hospital of Hunan Academy of Traditional Chinese Medicine, Changsha, 410006, People's Republic of China

Correspondence: Yongheng He, Department of Anorectal Surgery, Affiliated Hospital of Hunan Academy of Chinese Medicine, No. 58, Lushan Road, Yuelu District, Changsha, 410006, People's Republic of China, Tel +86-13517401858, Email He13517401858@163.com; Jingjing Wu, The Second Affiliated Hospital of Guangzhou University of Chinese Medicine, No. 111, Dade Road, Guangzhou, 510120, People's Republic of China, Tel +86-15989137849, Email wujingjing6028@gzucm.edu.cn

Background: Nasopharyngeal carcinoma (NPC) is a major global health issue, especially in Southeast Asia. Solamargine (SM), an alkaloid from natural plants, inhibits various cancer cells. This study evaluates SM's effects on invasion, migration, EMT markers, angiogenesis, and related pathways in the NPC-specific C666-1 cell line.

Methods: In vitro assays, including wound healing, Transwell invasion, Western blot, and tube formation, were used to assess SM's impact on C666-1 NPC and HUVEC cells. SM concentrations were 2 μM and 5 μM, with axitinib (4 μM) as the control. Network pharmacology and GO-KEGG enrichment analyses were conducted to explore SM's targets and mechanisms in NPC.

Results: SM significantly inhibited C666-1 NPC cell invasion and migration by reducing EMT markers Vimentin and Snail. In HUVEC cells, SM decreased viability, invasion, migration, and tube formation, likely through VEGF signaling inactivation, EZH2 inhibition, and miR-203a-3p upregulation. Network pharmacology and GO-KEGG analyses identified key targets and pathways, suggesting SM's anti-NPC effects through multiple mechanisms.

Discussion: SM inhibits NPC cell invasion and migration by regulating EMT, suppressing angiogenesis, and modulating key pathways. These findings highlight SM's potential as an anti-cancer agent for NPC and provide new insights into its mechanisms. Network pharmacology and GO-KEGG analysis further identify its therapeutic targets, offering valuable directions for future drug development.

Keywords: Nasopharyngeal carcinoma, solamargine, epithelial-mesenchymal transition, angiogenesis, network pharmacology

Introduction

Nasopharyngeal carcinoma (NPC) exhibits varying incidence rates globally, with a higher prevalence in East Asia and Southeast Asia due to regional genetic backgrounds, environmental factors, and unique dietary habits.[1,2] NPC spreads early and metastasize to other body parts, increasing the treatment complexity.[3–5] The primary pathogenic factors of this cancer include persistent infection with Epstein-Barr virus (EBV) and interactions with diverse environmental factors, forming a complex disease mechanism.[6–8] Clinically, NPC patients often miss the optimal treatment window due to late diagnosis and mild symptoms, leading to unfavorable outcomes.[9–11] Moreover, angiogenesis plays a crucial role in NPC development, supporting tumor growth and metastasis and becoming a research focus.[12,13] Active angiogenesis sustains rapid tumor growth by establishing an abnormal vascular network, primarily driven by various angiogenic factors secreted by cancer cells such as vascular endothelial growth factor (VEGF).[14–16]

Current NPC treatment methods mainly involve radiotherapy, chemotherapy, and surgery, yet these approaches often have significant limitations and side effects.[17–19] While radiotherapy remains a cornerstone treatment for NPC by effectively controlling local lesions, it may cause damage to surrounding healthy tissues, leading to post-treatment

Received: 24 October 2024
Accepted: 6 February 2025
Published: 8 April 2025

sequelae like swallowing difficulties and dry mouth.[18,20,21] Although chemotherapy can partly control systemic disease spread, its side effects, including nausea, vomiting, and leukopenia, cannot be overlooked.[22] Furthermore, activating the VEGF and its receptor pathways plays a critical role in NPC, posing a challenging obstacle to treatment by promoting endothelial cell growth, migration, and survival.[23] While several VEGF pathway inhibitors are approved for treating cancer and related diseases, the treatment outcomes vary among individuals, limiting the universal efficacy of anti-VEGF strategies.[24–26]

Solamargine (SM), a natural compound extracted from the eggplant plant, shows promising application prospects in cancer research.[27] Through various mechanisms, such as modulating apoptosis-related proteins, inhibiting cell cycle progression, and intervening in specific signaling pathways, SM effectively inhibits the growth and metastasis of multiple cancer cells.[28,29] In models like liver cancer and breast cancer, SM demonstrates apoptotic and autophagic induction actions, partly achieved through its regulation of the LIF/miR-192-5p/CYR61/Akt signaling pathway.[30–32] Additionally, the impact of SM on the immunostimulatory tumor microenvironment, particularly its role in modulating factors associated with tumor growth and metastasis, is a crucial aspect of research into its candidacy as an anticancer drug.[33] Preliminary experimental data in NPC research indicates that SM effectively inhibits the interaction of lncRNA CCAT1, miR-7-5p, and SP1, revealing its potential as a therapeutic approach against NPC.[34]

This study extensively explores the application potential of solamargine in NPC treatment, focusing on its impact on angiogenesis and metastasis processes. miR-203a-3p is a microRNA that inhibits tumor proliferation, migration, and invasion, while promoting apoptosis,[35] making it a potential therapeutic target. Notably, in retinal degeneration models, miR-203a-3p suppresses angiogenesis by targeting VEGFA, HIF-1α, and LncRNA MALAT1.[36,37] Given its potential role in angiogenesis inhibition, this study aims to evaluate whether SM can suppress NPC cell invasion and migration through modulation of these pathways. Through detailed in vitro experiments and meticulous molecular-level analysis, we aim to elucidate the specific mechanisms of SM on NPC angiogenesis and how it modulates the tumor microenvironment to slow down or prevent disease progression. These research findings are expected to provide new perspectives and strategies for the clinical treatment of NPC, especially when traditional treatment modalities are limited, offering more effective treatment options.

Materials and Methods

Cell Culture and Treatment

NPC cells C666-1 and HNE2, as well as primary human umbilical vein endothelial cells (HUVEC), were obtained from Sun Yat-sen Memorial Hospital in Guangzhou, Guangdong, China. C666-1 cells were cultured in RPMI-1640 medium (11875101, Gibco, USA) containing 10% fetal bovine serum (16140089, Gibco, USA) and 1% penicillin-streptomycin solution (15140148, Gibco, USA). HNE2 cells were maintained in DMEM medium (11966025, Gibco, USA) supplemented with 10% fetal bovine serum (16140089, Gibco, USA) and 1% penicillin-streptomycin solution (15140148, Gibco, USA). HUVEC cells were cultured in an endothelial cell basal medium supplemented with endothelial cell growth supplements. All cell lines were incubated at 37°C in a humidified atmosphere with 5% CO_2. Dimethyl sulfoxide (DMSO) (20688, Pierce, USA) was used to dissolve SM (C45H73NO15, purity ≥98%, Chengdu Maisto Biotechnology Co., China) and Axitinib (S1005, Selleck, USA), which were diluted to working concentrations prior to use. Axitinib, a receptor tyrosine kinase inhibitor, can inhibit the autophosphorylation of VEGFR and modulate VEGF-induced endothelial cell viability, tubule formation, and downstream signaling pathways.[38]

CCK-8 Assay for Cell Viability

Human umbilical vein endothelial cells (HUVECs) were seeded in a 96-well culture plate at a density of 5×10^3 cells per well. After incubating at 37°C with 5% CO_2 for 24 hours for adherence, cells were treated with varying concentrations of SM. Following treatment, 10 μL of CCK-8 solution (C0037, Biyuntian Biotech, China) was added to each well to ensure thorough mixing with the culture medium. The plate was then further incubated at 37°C with 5% CO_2 for 1 hour to allow the CCK-8 solution to react with the cells, producing a quantifiable color product. After the incubation period, the

absorbance (OD value) of each well at a wavelength of 450 nm was measured using a microplate reader to assess the impact of SM on HUVEC cell viability.

Cell Cloning Experiment

A starting density of 500 human Umbilical Vein Endothelial Cells (HUVEC) per well was seeded in a 6-well culture plate. In line with reported research, SM at concentrations of 2μM or 5μM effectively inhibited NPC cell growth.[34] Axitinib, a well-recognized VEGF receptor inhibitor, is widely used in anti-angiogenesis research.[39] Therefore, axitinib (4 μM) was included as a positive control in this study. Once the cells reached stable growth after seeding, they were treated with 5μM SM and cultured for 9 days to ensure that most individual clones contained more than 50 cells. During this period, the culture medium was replaced every three days, and regular observations of cell growth status were conducted. Upon achieving the desired clone count, cells were gently washed once with Phosphate-Buffered Saline (PBS) to remove the residual culture medium. Subsequently, a 4% paraformaldehyde solution was added to each well to fix the cells for 30 minutes, followed by another wash with PBS to remove the fixative. Post-fixation, the cells were stained with crystal violet staining solution for subsequent clone counting, and multiple washes with PBS were performed to remove unbound dye. After completion of the staining and washing steps, the cells were air-dried at room temperature, and then clones were counted in at least three different fields of view using a microscope produced by Nikon (Tokyo, Japan) to assess the efficiency and quality of clone formation.

EdU Incorporation Experiment

The Cell-Light™ EdU DNA Cell Proliferation Assay Kit (C10310, RiboBio, Guangzhou, China) was employed to assess the proliferation capability of HUVEC cells. HUVEC cells were seeded in a 96-well culture plate at a density of 1×10^4 cells per well and allowed to adhere and grow for 24 hours at 37°C in a 5% CO_2 environment until reaching optimal growth conditions. Subsequently, these cells were treated with culture media containing different concentrations of SM (2μM and 5μM) to evaluate the impact of SM on HUVEC cell proliferation. After 24 hours, the original culture media was removed from the wells, and fresh culture media containing 50μM EdU was added to each well. The cells were then further incubated at 37°C in a 5% CO_2 environment for an additional 2 hours to facilitate the integration of EdU into the cellular DNA.

The cells were gently washed twice with phosphate-buffered saline (PBS) to remove unincorporated EdU and other debris. Subsequently, the cells were treated with a 0.5% Triton X-100 solution for 10 minutes to increase the permeability of the cell membrane. The cells were then labeled with 1× Apollo staining reagent for 30 minutes to visualize cells incorporating EdU. In addition, the cellular DNA was counterstained with Hoechst 33342 for 30 minutes to label the nuclei of all cells.

Five random fields were selected for cell imaging using a fluorescence microscope (produced by Nikon, Tokyo, Japan) at 400× magnification. By calculating the ratio of EdU-positive cells to all Hoechst-stained cells, the proliferative capacity of the cells could be quantitatively assessed. The percentage of EdU-positive cells was calculated as follows: EdU-positive cell percentage = (EdU-positive cells/total Hoechst-stained cells) × 100.

MicroRNA Transfection Experiment

Mimics of miR-203a-3p, corresponding negative controls, and inhibitors were purchased from Guangzhou Ribobio Biotechnology Co., Ltd (miR10000264-1-5). These molecules were designed to modulate the expression levels of miR-203a-3p within cells, where mimics enhance the functionality of miR-203a-3p, while inhibitors serve to reduce its activity. Initially, HUVEC cells were seeded under suitable culture conditions to achieve a cell confluence of 70% to 80%. The aforementioned miRNA molecules (at concentrations of 50nM and 100nM) were transfected into the cells using appropriate transfection reagents. Following transfection, cells were further incubated in a culture chamber. After 30 hours post-transfection, the cells were treated with a predetermined concentration of SM for 24 hours. The addition of SM aimed to investigate further the role of miR-203a-3p in specific biological pathways and its impact on the cellular response induced by SM.

Cell Co-Culture Experiment

In order to investigate the effects of SM and Axitinib on nasopharyngeal carcinoma cell line (C666-1) on the growth of HUVECs, C666-1 cells were first treated in a culture medium containing appropriate concentrations of SM and Axitinib for 24 hours. Subsequently, cells underwent starvation treatment for 24 hours by culturing them in a serum-free medium to reduce extracellular signaling and more accurately assess the impact of SM and Axitinib on C666-1 cells. After starvation treatment, a conditioned medium (CM) from the treated C666-1 cells containing cell-secreted factors was collected. This CM was then mixed in a 1:1 ratio with fresh culture medium containing complete nutritional components to simulate the nutritional and signaling states in the tumor microenvironment while providing essential nutrients for the growth of HUVECs. Lastly, the aforementioned mixed culture medium was used to co-culture with HUVECs to study the influence of C666-1 cells under SM and Axitinib treatment on HUVEC behavior. During the co-culture period, subsequent assessments, such as cell proliferation, migration, and tube formation abilities, were conducted to evaluate the angiogenic potential of HUVECs.

Detection of Protein Expression by Western Blot Analysis

Cell lysis was performed using RIPA buffer containing protease inhibitors (20–188, Millipore, USA), and the protein concentration in the cell lysates was determined using the Quick Start™ Bradford Protein Assay Kit (5000201, BIO-RAD, USA). Subsequently, protein separation was carried out on 10% SDS-PAGE gels, then transferred onto a PVDF membrane (IPVH08100, Millipore, USA) using a semi-dry transfer apparatus. The PVDF membrane was blocked in 5% BSA for 1 hour and then incubated overnight at 4°C with primary antibodies against EZH2 (1:3000) (5246, Cell Signaling Technology, USA), VEGFR2 (1:1000) (2479, Cell Signaling Technology, USA), Snail (1:1000) (3879, Cell Signaling Technology, USA), Vimentin (1:1000) (5741, Cell Signaling Technology, USA), VEGFA (1:1000) (ab46154, Abcam, USA), β-Tubulin (1:1000) (2128, Cell Signaling Technology, USA), or β-Actin (1:5000) (4970, Cell Signaling Technology, USA). Following washing, the membrane was probed with an HRP-conjugated secondary antibody (1:4000) (7074, Cell Signaling Technology, USA) for 1 hour, and protein bands were detected using ECL solution (36208ES60, Yeasen Bio, Shanghai, China) with the ChemiDoc XRS Gel Imaging System from Bio-Rad.

Detection of miRNA and mRNA Levels Using RT-qPCR Experiment

RNA was extracted from collected samples using Trizol reagent (T9424, Sigma-Aldrich, USA). To analyze the expression patterns of miRNA, the first-strand cDNA was synthesized from the extracted RNA using the miRNA First Strand cDNA Synthesis Kit (MR101-01, Nanjing Novozymes, China). This kit is specifically designed for efficient reverse transcription of miRNA to cDNA, ensuring the accuracy and reproducibility of miRNA expression analysis. For the cDNA preparation in mRNA expression level analysis, Hiscript® III RT SuperMix (R323-01, Nanjing Novozymes, China) was utilized. This SuperMix contains optimized reverse transcriptase and reaction buffers to enhance the reverse transcription efficiency of mRNA and the overall accuracy of qPCR analysis. Real-time quantitative PCR (qPCR) analysis was performed using ChamQ Universal SYBR qPCR Master Mix (Q711-02, Nanjing Novozymes, China) and ABI ViiA7 Real-Time PCR System (Applied Biosystems, USA). All qPCR experiments followed the standard operating procedures provided by the manufacturer, with each sample undergoing at least three independent analyses to ensure data reproducibility and reliability. The primer sequences used in this study are listed in Table 1.

Scratch Assay to Assess Cell Migration

C666-1 and HUVEC cells were seeded in a 6-well plate and allowed to grow to confluency. Subsequently, a scratch wound was created in the monolayer of cells using the sterile tip of a 200 μL pipette. After wound formation, the cells were gently washed twice with PBS to remove any floating cells and debris. Next, the cells were further incubated for 16 hours in starvation media containing different concentrations of SM (2 μM and 5 μM) and Axitinib (4 μM). Cell migration was evaluated using an Olympus microscope (100×) with a high-definition digital camera. The experiment was independently repeated three times to ensure the reproducibility and statistical significance of the results.

Table 1 Primers Used in the Study

Gene Name	Forward/Reverse	Sequence
GAPDH	Forward	5'- CTCCTCCTGTTCGACAGTCAGC-3'
	Reverse	5'-CCCAATACGACCAAATCCGTT-3'
VEGFA	Forward	5'-TACCTCCACCATGCCAAGTG-3'
	Reverse	5'-ACTTCGTGATGATTCTGCCCTC-3'
HIF-1α	Forward	5'-CATAAAGTCTGCAACATGGAAGGT-3'
	Reverse	5'-ATTTGATGGGTGAGGAATGGGTT-3'
U6	Forward	5'- ATTGGAACGATACAGAGAAGATT-3'
	Reverse	5'-GGAACGCTTCACGAATTTG-3'
miR-203a-3p	Forward	5'-GUGAAAUGUUUAGGACCACUAG-3'
	Reverse	5'-AGUGGUCCUAAACAUUUCACUU-3'

Abbreviations: GAPDH,Glyceraldehyde-3-Phosphate Dehydrogenase; VEGFA, Vascular Endothelial Growth Factor A; HIF-1α,Hypoxia Inducible Factor 1 Subunit Alpha.

Transwell Assay for Cell Migration

To investigate the migratory ability of C666-1 and HUVEC cells, both cell lines were cultured in a serum-free medium for 12 hours to induce a state of starvation, thus minimizing the impact of external factors on cell migration. Subsequently, a diluted Matrigel matrix (356234, BD Biosciences, USA) was coated on the upper chamber of the Transwell device to mimic the extracellular matrix and facilitate cell migration. The lower chamber of the Transwell was filled with a culture medium containing 20% fetal bovine serum (FBS) as a chemoattractant to stimulate cell migration. C666-1 and HUVEC cells were suspended in a starvation medium containing specific treatment agents (SM and Axitinib), and approximately 1×10^5 cells were seeded into each well in the upper chamber. After a 24-hour incubation period, the cells in the lower chamber were fixed with 4% formaldehyde and stained with 0.1% crystal violet for subsequent observation and counting under a microscope. Six random fields of view (at 200x magnification) were selected, and cell counting was performed using a Nikon TI2-E microscope to assess changes in cell migration and invasiveness. This experimental procedure was independently repeated three times to ensure the reproducibility and accuracy of the results.

Formation of Tubular Structures for Testing the Angiogenic Ability of Cells

Matrigel was thawed at 4°C for 24 hours to ensure uniformity and removal of air bubbles. Subsequently, Matrigel was diluted with serum-free culture medium at a 1:2 ratio to accommodate the growth needs of HUVEC cells. 200μL of the diluted Matrigel was evenly distributed into each well of a 24-well plate and incubated at 37°C with 5% CO_2 for 2 hours to promote gelation, creating a three-dimensional matrix conducive to cell attachment and growth. Next, appropriately treated HUVEC cells were seeded at a density of 1.0×10^4 cells per well on the Matrigel-coated wells. Cells were then cultured for an additional 24 hours at 37°C with 5% CO_2 to allow for cell migration and interconnection within the Matrigel matrix, forming tube-like structures reminiscent of blood vessels. To quantitatively analyze the formation of tubular structures, each well was examined and imaged under an Olympus microscope at 100x magnification. Three random fields of view were selected per well to ensure data representativeness and repeatability. The number of nodes in the selected fields was calculated to assess the angiogenic capacity of HUVEC cells.

Acquisition of Drug Active Targets and Screening of Disease Targets

Initially, a search was conducted on the active ingredient Solamargine of Datura metal through the Chinese Systems Pharmacology Database and Analysis Platform (TCMSP, https://old.tcmsp-e.com/tcmsp.php) and the BATMAN-TCM database (http://bionet.ncpsb.org.cn/batman-tcm/index.php) to collect information on its corresponding targets. Subsequently, the GeneCards database (https://www.genecards.org/) was accessed, and a search was performed using "nasopharyngeal carcinoma" as a keyword to screen for targets related to this disease.

Protein-Protein Interaction (PPI) Network Analysis

A Protein-Protein Interaction (PPI) network was constructed using the String database (https://cn.string-db.org/) to identify interactions between predicted targets of Solamargine, an active compound, and disease targets associated with nasopharyngeal carcinoma. A confidence threshold of 0.4 was set to ensure the reliability of interactions within the network.

GO and KEGG Pathway Enrichment Analysis

The common targets of Solamargine and nasopharyngeal carcinoma were subjected to GO functional enrichment and KEGG pathway enrichment analysis using the online tool Metascape. A significance threshold of $P < 0.05$ was set to identify biologically relevant processes, cellular components, molecular functions, as well as metabolic or signaling pathways that may be implicated in drug action.

Topology Analysis Using Cytoscape and CytoNCA

The PPI network was imported into Cytoscape software for topological analysis. The CytoNCA plugin was employed to conduct centrality analysis within the network, aiming to identify critical nodes or central targets. By analyzing betweenness centrality and closeness centrality, crucial protein targets were selected to unveil their pivotal roles in the antitumor process of Solamargine against nasopharyngeal carcinoma.

Statistical Analysis

The data from at least three independent experiments were presented as Mean ± SD and analyzed using one-way ANOVA and Student's *t*-test (GraphPad Prism 5.0, GraphPad Software, USA). All statistical comparisons were conducted between the experimental and corresponding control groups, with significance levels indicated by asterisks. A p-value < 0.05 was considered statistically significant.

Results

SM Inhibits Invasion and Migration of C666-1 Nasopharyngeal Carcinoma Cells by Modulating Epithelial-Mesenchymal Transition (EMT) Markers

Results from Transwell invasion and scratch assays demonstrated that SM significantly suppressed the migration and invasion capabilities of C666-1 cells (Figure 1A and B). Furthermore, Western blot analysis revealed that SM reduced the expression of EMT-associated proteins Vimentin and Snail, indicating that SM may inhibit the invasion and migration of NPC cells by modulating the EMT process (Figure 1C and D). Cell migration, invasion capabilities, and marker protein expression levels were quantitatively analyzed through microscopic cell counting and grayscale analysis of protein bands (Figure 1E). Axitinib, used as the positive control, similarly exhibited inhibitory effects on C666-1 cells, further confirming the efficacy of SM as a potential candidate for anticancer therapy.

Study on the Inhibitory Effect of SM on Angiogenic Function of HUVEC Cells

Through a series of in vitro experiments, this research assessed the influence of SM on the vascular formation capability of HUVEC cells. The impact of SM on HUVEC cell viability was initially observed using the CCK-8 assay. The results indicate that SM significantly inhibits the activity of HUVEC cells, with the dose-dependent inhibitory effect being similar to what was previously observed in NPC cells (Figure 2A). The EdU staining experiment evaluated the effect of SM on the proliferative capacity of HUVEC cells, demonstrating that SM effectively suppresses HUVEC cell proliferation, albeit slightly less than the positive control group CON (treated with the anti-cancer drug, axitinib) (Figure 2B). Additionally, the study employed Transwell, scratch, and tube formation assays to further investigate the impact of SM on the invasion, migration, and tubular structure formation abilities of HUVEC cells. As illustrated in Figure 2C–E, SM treatment significantly hinders the invasion and migration of HUVEC cells and tube formation, with the inhibitory effect comparable to the positive control drug axitinib. Cell migration and invasion abilities were quantitatively analyzed through microscopic cell counting and protein band grayscale analysis (Figure 2F).

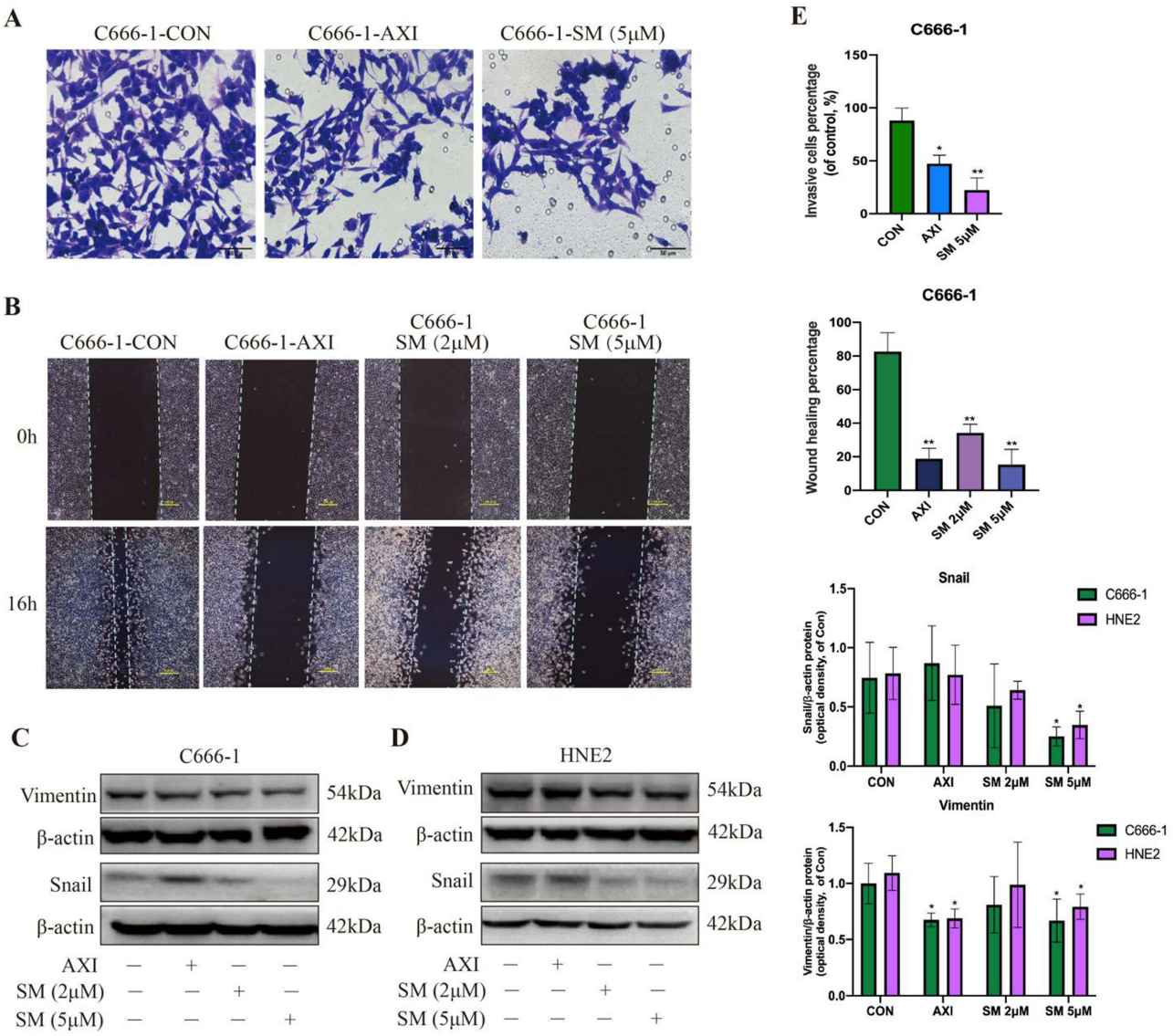

Figure 1 SM Inhibits Invasion and Migration of C666-1 Cells.

Note: (**A**) Transwell experiment to evaluate the impact of 5μM SM on the migration of C666-1 cells. (**B**) Wound healing assay investigating the effects of different concentrations of SM (2μM and 5μM) on the invasive ability of C666-1 cells. (**C** and **D**) Western blot analysis of Vimentin and Snail protein expression in C666-1 and HNE2 cells treated with varying concentrations of SM (2μM and 5μM). (**E**) Quantitative analysis and graphical representation of cell migration, scratch assay, and Western blot results were conducted through cell counting and analysis of Western blot protein band grayscale values. All cell experiments were performed in triplicate, with data presented as mean ± standard deviation. *: $P < 0.05$, **: $P < 0.01$ compared to the control (CON) group.

SM Suppresses Angiogenic Capacity of HUVEC Cells by Inactivating VEGF Signaling Pathway and Upregulating miR-203a-3p

Our results demonstrate that SM treatment leads to the inactivation of the VEGF signaling pathway, including the downregulation of VEGFA, VEGFR2, and HIF-1α, thereby inhibiting the angiogenic ability of ECs (Figure 3A–C). Furthermore, we noticed that SM could suppress the expression of EZH2, a critical transcription factor involved in cancer angiogenesis and metastasis. Inhibition of EZH2 by SM treatment further impacts the angiogenic process. Importantly, we discovered that SM treatment upregulates the expression of miR-203a-3p in HUVEC cells (Figure 3D).

https://doi.org/10.2147/JIR.S485244

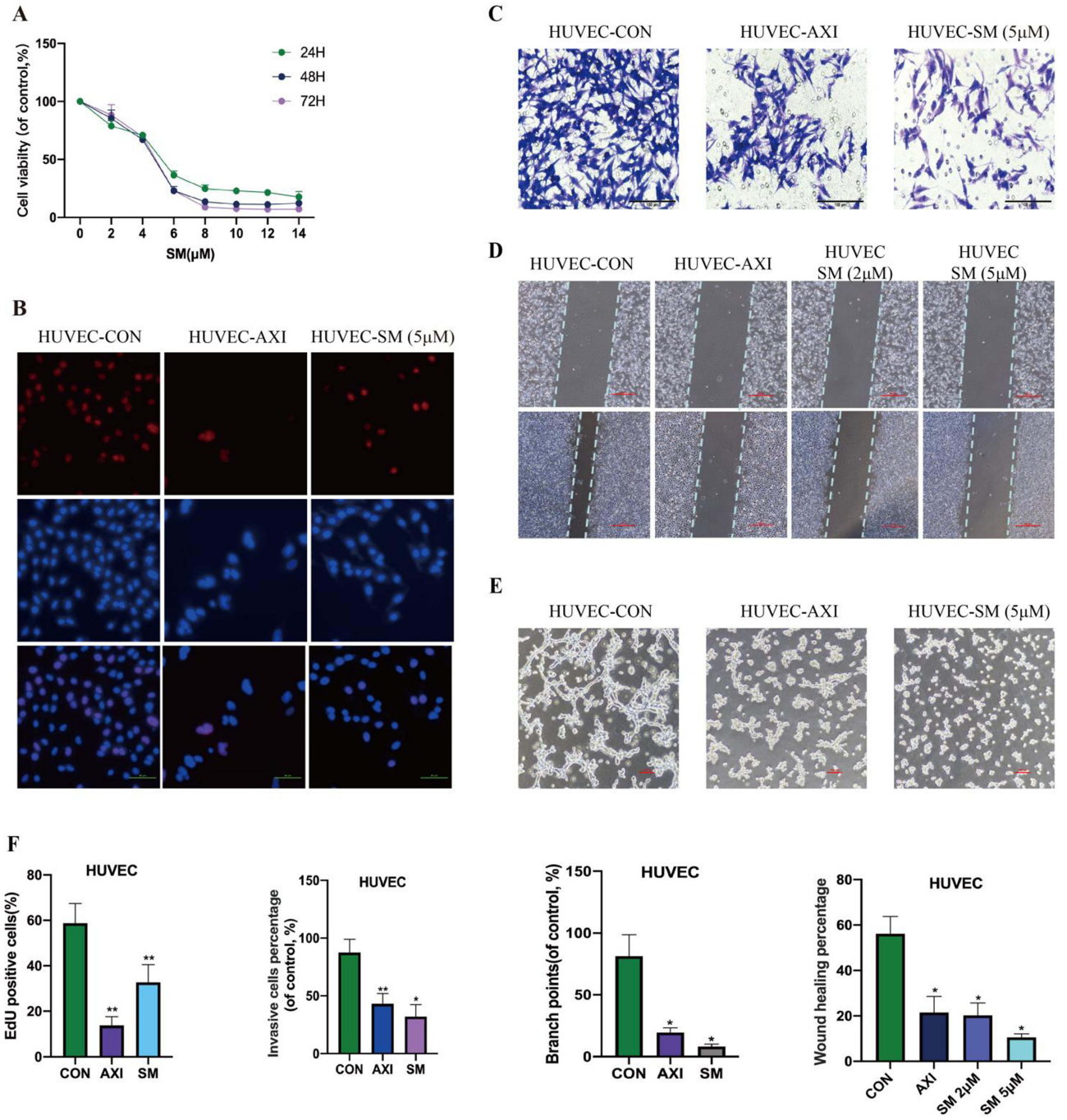

Figure 2 The Inhibitory Effect of SM on the Growth, Invasion, Migration, and Tube Formation of HUVEC Cells.
Note: (**A**) Cell viability of HUVEC cells treated with SM was assessed using CCK-8 assay. (**B**) EdU analysis was performed to evaluate the proliferation of HUVEC cells (scale bar: 50 μm). (**C** and **D**) Transwell and scratch assays were employed to assess the migration and invasion of HUVEC cells under SM treatment. (**E**) Tube formation assay was conducted to evaluate the tube formation ability of HUVEC cells. (**F**) Quantitative analysis of cell proliferation, migration, and invasion experiments was performed. All cell experiments were repeated three times. *: $P<0.05$, **: $P<0.01$ compared to the CON group.

Impact of SM on HUVEC Tube Formation Induced by C666-1 Cells and Related Molecular Expression

The conditioned medium from C666-1 cells was collected and co-cultured with HUVEC cells to mimic angiogenesis in the tumor microenvironment. The experimental results indicate that the conditioned medium of C666-1 cell culture significantly enhanced the tube formation of HUVEC cells, an effect that was notably diminished upon SM treatment (Figure 4A).

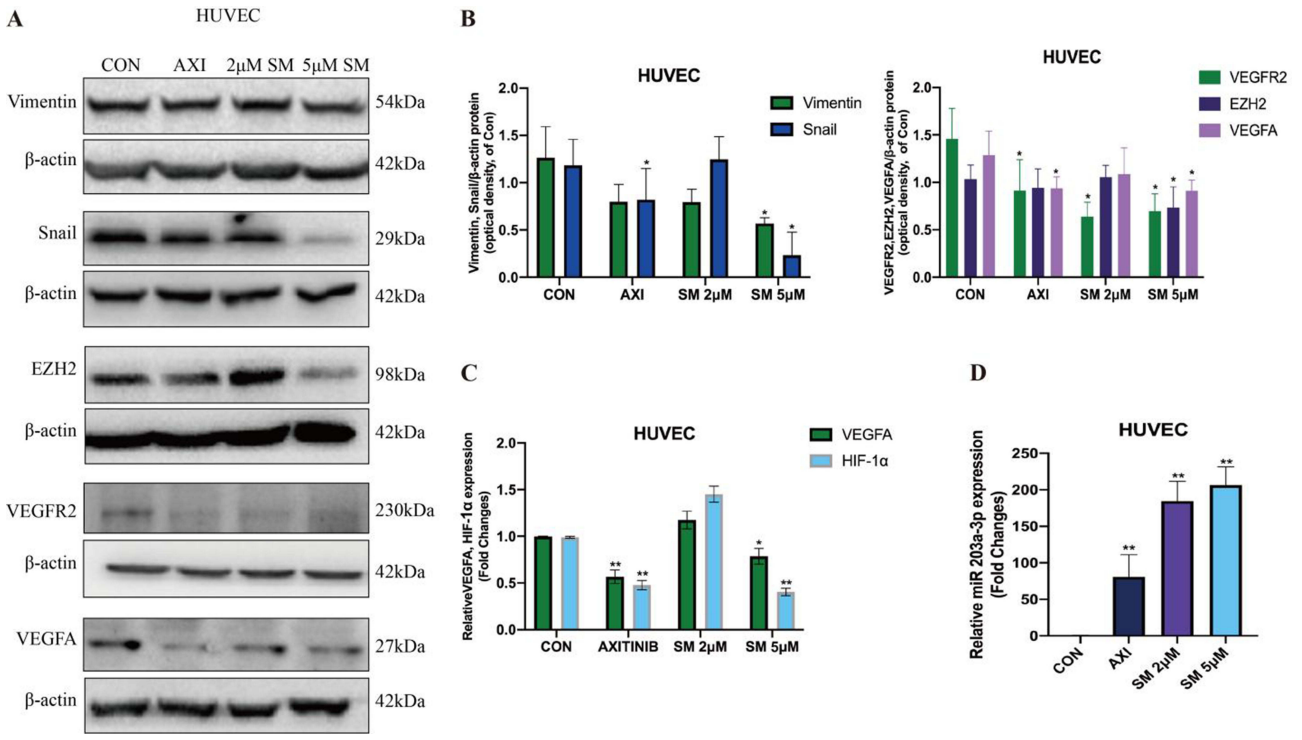

Figure 3 SM Regulation of VEGF Signaling Pathway and miR-203a-3p Expression in HUVEC Cells.
Note: (**A**) Changes in the EMT markers and VEGF signaling pathway in HUVEC cells after SM treatment were assessed using Western blot analysis. (**B**) Analysis of protein band grayscale values by Western blot. (**C** and **D**) q-RT-PCR analysis of the levels of VEGFA, HIF-1α mRNA, and miR-203a-3p in HUVEC cells after SM treatment (scale bar: 50 μm). All cellular experiments were replicated three times. *: $P < 0.05$, **: $P < 0.01$, significant differences compared to the CON group.

Furthermore, molecular analysis revealed that the conditioned medium of C666-1 culture promoted the expression of EZH2, VEGFR2, and VEGFA proteins (Figure 4B and C) while simultaneously reducing the expression of miR-203a-3p (Figure 4D). In contrast to the expression pattern induced by the conditioned medium of C666-1 culture, SM treatment significantly suppressed the expression of EZH2, VEGFR2, and VEGFA while increasing the levels of miR-203a-3p.

MiR-203a-3p Modulates the Regulatory Effects of SM on HUVEC Angiogenesis by Regulating EZH2 and VEGFA Expression

Experimental findings demonstrated that miR-203a-3p mimics significantly inhibited HUVEC cell viability and enhanced the inhibitory effects of SM on HUVEC cell growth, while miR-203a-3p inhibitors promoted cell growth. Furthermore, SM was able to neutralize the pro-growth effects induced by the inhibitors in HUVEC cells (Figure 5A). These findings are consistent with previous studies indicating that miR-203a-3p inhibits VEGFA and HIF-1α expression by targeting their 3'UTR. This study further confirmed that miR-203a-3p mimics decreased the protein expression of EZH2 and VEGFA (Figure 5B), whereas inhibitors increased the expression of these proteins (Figure 5C). Importantly, SM also suppressed the induction of EZH2 and VEGF expression by the inhibitors in HUVEC cells (Figure 5D).

Interactions Between SM and NPC: Network Pharmacology Analysis

In order to delve into the potential mechanisms of Solamargine (SM) against NPC, this study utilized network pharmacology methods (Figure 6A) to predict and analyze the interaction targets of SM with NPC. Initially, a search in the TCMSP and BATMAN-TCM databases was conducted for target identification related to "SM", resulting in identifying 27 known and predicted targets. Subsequently, using the GeneCards and OMIM databases, 2882 and 193 NPC-related targets were identified, respectively. Following deduplication, a total of 3015 NPC-related targets were consolidated. Through the intersection analysis of the 27 SM and 3015 NPC targets, 20 common targets potentially

https://doi.org/10.2147/JIR.S485244

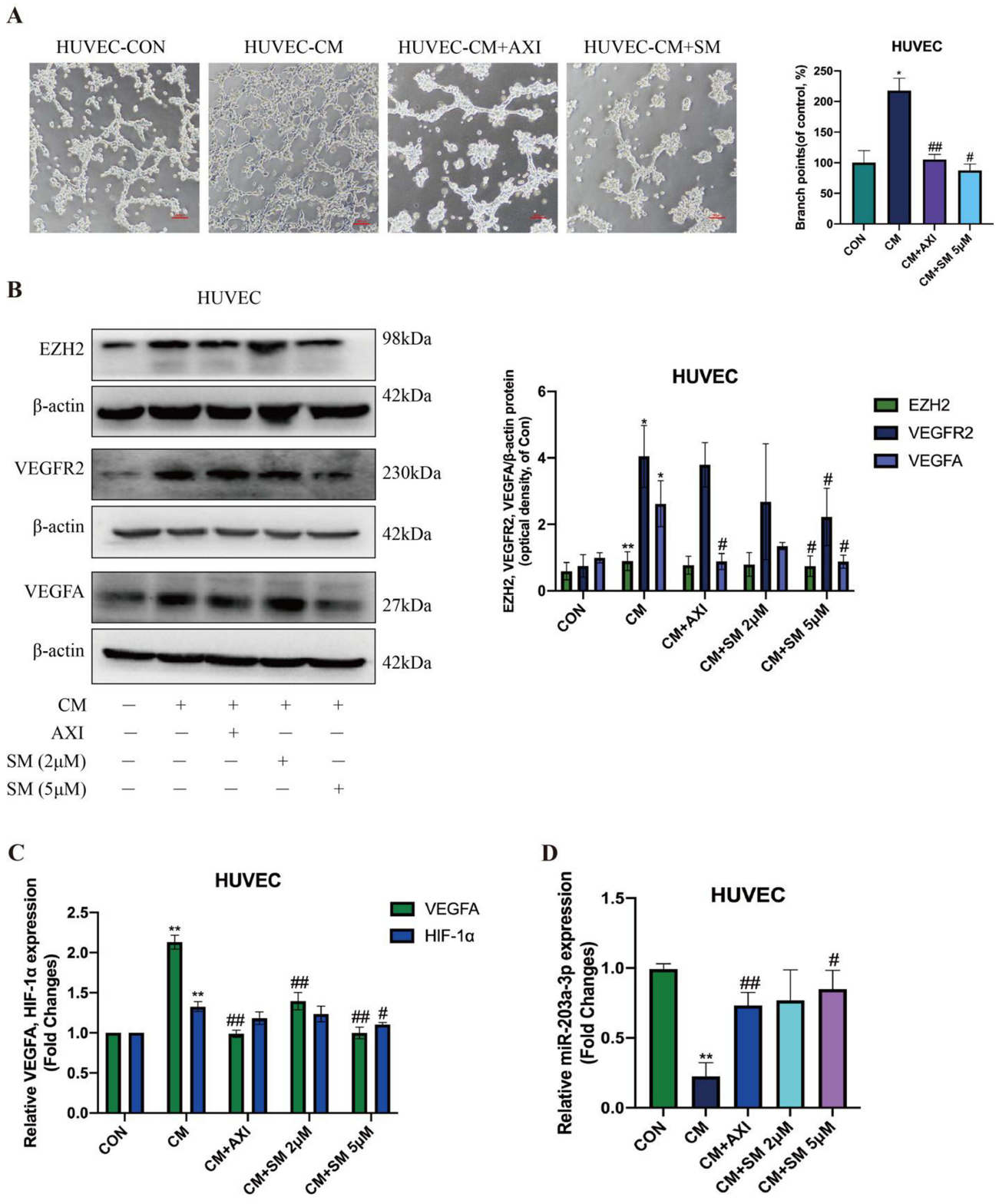

Figure 4 Stimulation of Tube Formation in HUVEC Cells by Secretion of Pro-Angiogenic Factors from C666-1 Cells.

Note: (**A**) Tube formation experiments were conducted to measure the effects of conditioned media from C666-1 cells (with or without SM) on tube formation in HUVEC cells. (**B**) Expression of EZH2, VEGFR2, and VEGFA proteins was assessed by Western blot. (**C** and **D**) Expression of VEGFA, HIF-1α, and miR-203a-3p was evaluated using qRT-PCR. All cellular experiments were repeated three times. *: $P < 0.05$, **: $P < 0.01$ significant difference compared to the CON group. #: $P < 0.05$, ##: $P < 0.01$ significant difference compared to the CM group.

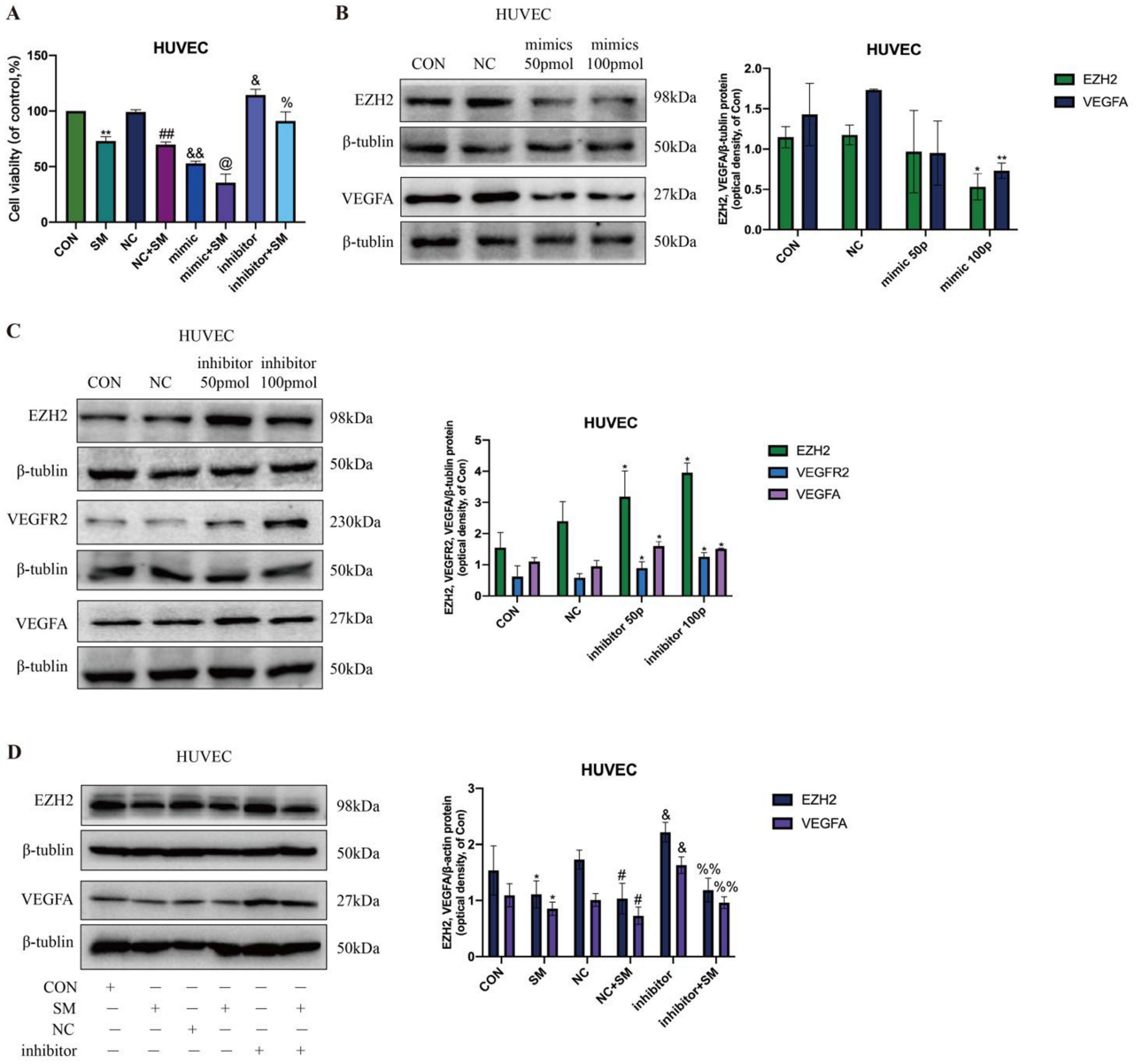

Figure 5 Regulatory Effects of miR-203a-3p on EZH2 and VEGFA Expression in SM-Treated HUVEC Cells.

Note: (**A**) Impact of miR-203a-3p mimics and inhibitors on the viability of HUVEC cells post-SM treatment. (**B**) Influence of miR-203a-3p mimics on the protein levels of EZH2 and VEGFA in HUVEC cells. (**C**) Effect of miR-203a-3p inhibitors on the protein levels of EZH2 and VEGFA in HUVEC cells. (**D**) SM suppresses the induced upregulation of EZH2 and VEGFA expression by miR-203a-3p inhibitors. All cell experiments were repeated three times. *: P < 0.05, **: P < 0.01, indicating significant differences compared to the CON group. #: *P* < 0.05, ##: *P* < 0.01, indicating significant differences compared to the NC group. &: *P* < 0.05, &&: *P* < 0.01, indicating significant differences compared to the NC group. @: *P* < 0.05, indicating significant differences compared to the mimic group. %: *P* < 0.05, %%: *P* < 0.01, indicating significant differences compared to the inhibitor group.

involved in the anti-NPC effects of SM were identified (Figure 6B). Employing the PPI network constructed using the String database with a confidence level of 0.400, the network comprised 20 nodes and 73 edges. Enrichment analysis of the PPI network indicated a p-value less than 1.33e-05, confirming the statistical significance of the network. Topological analysis was conducted using Cytoscape in conjunction with CytoNCA, and based on the Betweenness Centrality criterion, 10 core targets were determined, namely ACTB, TNF, AKT1, CASP3, ACTC1, TFRC, BCL2, ACTA1, PKM, and ACTG1 (Table 2, Figure 6C).

https://doi.org/10.2147/JIR.S485244

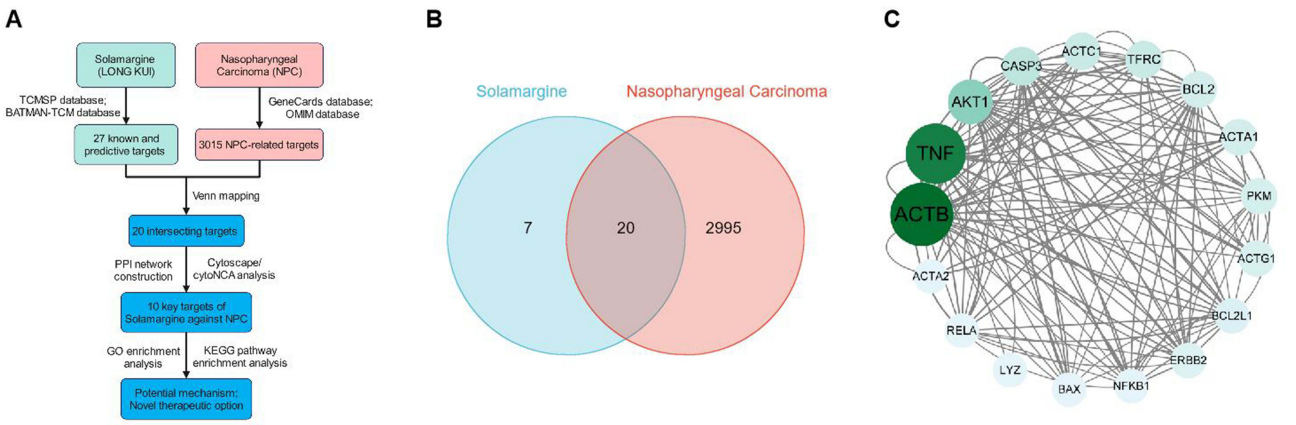

Figure 6 Network Pharmacology Analysis of the Interaction Targets between SM and NPC.
Note: (**A**) Workflow of the network pharmacology analysis of the interaction targets and pathways between SM and NPC; (**B**) Venn diagram showing the shared targets between SM and NPC; (**C**) Analysis of the target interactions between SM-NPC using String and Cytoscape/CytoNCA.

GO-KEGG Enrichment Analysis of SM Target Genes in NPC Reveals Potential Therapeutic Mechanisms

This study comprehensively analyzed the core target interaction between SM and NPC through gene ontology (GO) and Kyoto Encyclopedia of Genes and Genomes (KEGG) pathway enrichment analysis. It delved into the potential biological processes, cellular components, and molecular functions underlying the anti-NPC effects of SM, as well as related biological metabolism and signaling pathways (Table 3).

In the Biological Process (BP) category, Figure 7 illustrates significant enrichments in processes such as "striated muscle cell differentiation" (GO:0051146), "response to metal ion" (GO:0010038), "muscle cell differentiation" (GO:0042692), and "response to decreased oxygen levels" (GO:0036293). It indicates that SM may exert its anti-NPC effects by modulating specific cell differentiation pathways and responses to environmental changes. In the Cellular Component (CC) category, notably enriched terms include "blood microparticles" (GO:0072562), "actin filaments" (GO:0005884), and "leading edge membrane" (GO:0030027), suggesting that SM may intervene in the physical properties and intercellular communication of NPC cells by affecting the cell cytoskeleton and extracellular components. The Molecular Function (MF) category analysis highlights the significance of functions such as "cellular cytoskeleton structure" (GO:0005200) and "protein binding"

Table 2 Paramters of Top-10 Key Targets from Network Nodes

Targets	Betweenness Centrality	Closeness Centrality
ACTB	45.535713	0.3272727
TNF	40.769047	0.31578946
AKT1	16.369047	0.31578946
CASP3	7.202381	0.31034482
ACTC1	4.8333335	0.2769231
TFRC	4.766667	0.29032257
BCL2	3.2690477	0.30508474
ACTA1	3.1666667	0.27272728
PKM	2.6	0.29508197
ACTG1	2.1190476	0.2769231

Note: Targets were ranked by Betweenness Centrality analyzed using cytoNCA.
Abbreviations: ACTB, β - actin; TNF, Tumor Necrosis Factor; AKT1, AKT Serine/Threonine Kinase 1; CASP3, Caspase-3; ACTC1, Cardiac α-Actin; TFRC, Transferrin Receptor; BCL2, B-Cell Lymphoma 2; ACTA1, Skeletal Muscle Alpha-Actin; PKM, Pyruvate Kinase M; ACTG1, Gamma-Actin.

Table 3 GO-KEGG Enrichment Analysis for Key Targets of Solamargine Against NPC

Ontology	ID	Description	GeneRatio	p value	p.adjust
BP	GO:0051146	Striated muscle cell differentiation	6/10	2.11e-09	3.19e-06
BP	GO:0010038	Response to metal ion	6/10	8e-09	6.05e-06
BP	GO:0042692	Muscle cell differentiation	6/10	1.43e-08	7.22e-06
BP	GO:0033138	Positive regulation of peptidyl-serine phosphorylation	4/10	2.03e-07	7.02e-05
BP	GO:0036293	Response to decreased oxygen levels	5/10	2.32e-07	7.02e-05
CC	GO:0072562	Blood microparticle	5/10	5.43e-09	5.05e-07
CC	GO:0005884	Actin filament	4/10	2.14e-07	9.97e-06
CC	GO:0030027	Lamellipodium	4/10	2.19e-06	6.8e-05
CC	GO:0005869	Dynactin complex	2/10	2.8e-05	0.0006
CC	GO:0044305	Calyx of Held	2/10	3.57e-05	0.0006
MF	GO:0005200	Structural constituent of cytoskeleton	3/10	2.04e-05	0.0009
MF	GO:0099186	Structural constituent of postsynapse	2/10	2.06e-05	0.0009
MF	GO:0098918	Structural constituent of synapse	2/10	4.52e-05	0.0009
MF	GO:0002020	Protease binding	3/10	4.56e-05	0.0009
MF	GO:0032813	Tumor necrosis factor receptor superfamily binding	2/10	0.0003	0.0051
KEGG	hsa04210	Apoptosis	6/9	1.54e-09	2.52e-07
KEGG	hsa05132	Salmonella infection	6/9	5.9e-08	4.81e-06
KEGG	hsa05418	Fluid shear stress and atherosclerosis	5/9	1.59e-07	8.63e-06
KEGG	hsa05164	Influenza A	5/9	4.48e-07	1.82e-05
KEGG	hsa05205	Proteoglycans in cancer	5/9	1.1e-06	3.6e-05

Abbreviations: BP, Biological Process; CC, Cellular Component; MF, Molecular Function; KEGG, Kyoto Encyclopedia of Genes and Genomes.

(GO:0002020), indicating that SM regulates the survival and proliferation of NPC cells through these molecular functions. KEGG pathway analysis reveals that signaling pathways like "apoptosis" (hsa04210), "salmonella infection" (hsa05132), and "fluid shear stress and atherosclerosis" (hsa05418) may play crucial roles in SM's treatment of NPC.

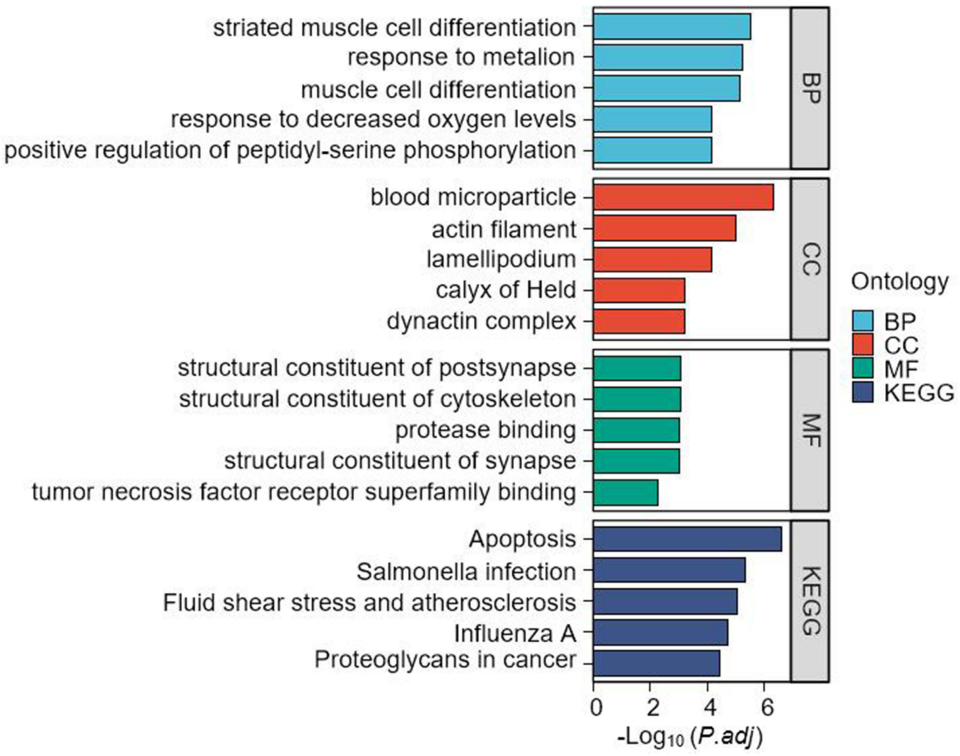

Figure 7 Enrichment Analysis of SM on NPC Targets Reveals Potential Therapeutic Mechanisms.

https://doi.org/10.2147/JIR.S485244

Discussion

This study demonstrates that SM significantly inhibits the migration and invasion of NPC cells by reducing the key EMT markers Vimentin and Snail. This finding is consistent with previous research on other anticancer drugs, such as Gefitinib, which also modulates EMT markers, but SM exhibits certain unique mechanisms.[40,41] Unlike relying solely on the common cytotoxicity of anti-tumor drugs, SM appears to achieve its inhibitory effects through more refined molecular regulatory pathways, like directly modulating the activity of specific transcription factors.[42–44] Furthermore, the action of SM on NPC cells may also involve influencing intracellular signaling, a less common phenomenon in previous EMT-related treatment studies.[45,46] Therefore, the unique anti-metastatic properties of SM offer a new perspective for NPC treatment and may also present potential therapeutic avenues for other tumors with EMT characteristics.[47,48]

Regarding angiogenesis, experimental results on HUVEC cells show that SM significantly inhibits cell viability, invasion, migration, and tubular structure formation.[49–51] This effect is similar to anti-angiogenic drugs currently used, such as Axitinib, but SM demonstrates uniqueness in its mechanism of action, affecting not only the VEGF signaling pathway but also involving other molecules like EZH2 inhibition and upregulation of miR-203a-3p.[52] It suggests that SM may influence angiogenesis through a multi-signaling pathway network, offering potential advantages in treatment by targeting multiple points.[53–55] In comparison to conventional therapies, the multifaceted intervention of SM may enhance its ability to combat NPC angiogenesis while potentially reducing issues of drug resistance stemming from reliance on a single target.[47,48]

Within its anti-tumor activity, the impact of SM on the VEGF signaling pathway is particularly crucial.[56,57] The VEGF signaling pathway is a key regulator of angiogenesis and has been shown to promote tumor growth and metastasis in various cancers.[58,59] In this study, SM significantly inhibits the invasiveness of NPC cells and the angiogenic potential of HUVEC by deactivating this pathway. This finding aligns with previous research, as several studies have reported that anti-VEGF therapies effectively suppress tumor angiogenesis and metastasis.[60–62] However, while regulating the VEGF pathway, SM also involves other signals, such as EZH2 and miR-203a-3p modulation, potentially explaining its complex and diverse effects in inhibiting tumorigenesis.[43,63,64] This multi-layered signaling regulation strategy may provide a new approach to addressing the issues of drug resistance and side effects in current anti-VEGF therapies.[53,65,66]

miR-203a-3p is crucial in various biological processes, including cell proliferation, migration, and angiogenesis.[67,68] In this study, SM upregulates miR-203a-3p to inhibit NPC angiogenesis and metastasis, consistent with the mechanism of action of miR-203a-3p in other cancer treatments, such as in breast and liver cancer studies where upregulation of miR-203a-3p is associated with tumor growth inhibition. However, further molecular-level research is needed to elucidate how precisely SM regulates miR-203a-3p and how this regulation intricately affects the pathological processes of NPC.[69,70] Additionally, exploring the interaction of miR-203a-3p with the specific signaling network of NPC will contribute to a more comprehensive understanding of SM's anticancer mechanisms.[71]

Through network pharmacology and GO-KEGG pathway enrichment analysis, this study unveils the core targets of SM interacting with NPC and the related biological metabolism and signaling pathways. AKT1, a serine/threonine protein kinase, as a crucial component of the PI3K/AKT signaling pathway, regulates the expression of angiogenic factors such as nitric oxide and vascular endothelial growth factor. Activation of AKT1 has been reported to induce the generation of structurally abnormal vessels and distortion of tumor vasculature,[72] promoting the survival of NPC tumor cells and resistance to cell apoptosis.[73] PKM (Pyruvate Kinase M) is a key enzyme in the glycolysis process, and its isoform PKM2 can translocate to the nucleus to influence the activity of HIF-1α (hypoxia-inducible factor 1α), a crucial transcription factor in angiogenesis, by promoting the expression of VEGF and other angiogenesis-related genes.[74]

Furthermore, ACTB (Beta-Actin) plays a crucial role in cellular skeletal composition and movement. Aberrant expression of ACTB may affect the migratory and invasive capabilities of NPC tumor cells.[75] TNF (Tumor Necrosis Factor) is an important regulator of inflammation and immune response, exerting anticancer effects by promoting cell apoptosis and inhibiting tumor growth. However, prolonged TNF signaling may lead to tumor environment inflammation, thereby promoting tumor growth and metastasis.[76] CASP3 (Caspase-3) is a key enzyme in the execution phase of cell apoptosis, participating in the cell death signaling pathway. Activation of CASP3 may be an effective strategy to induce tumor cell death.[77] Aberrant

expression of ACTC1 (Cardiac α-Actin) in some cancers is associated with tumorigenesis and progression. TFRC (Transferrin Receptor) is involved in iron uptake and regulation; iron is essential in many cellular metabolic processes. Increased TFRC expression may promote tumor growth.[78,79] BCL2 (B-Cell Lymphoma 2) is an anti-apoptotic protein that promotes tumor cell survival by inhibiting cell death. In NPC, overexpression of BCL2 may be associated with chemotherapy resistance. ACTA1 (Skeletal Muscle Alpha-Actin) expression is typically associated with muscle tissue and may impact the mobility and invasiveness of tumor cells.[80] ACTG1 (Gamma-Actin) participates in the assembly and remodeling of the cellular skeleton, crucial for maintaining cell morphology and facilitating cell movement. The role of ACTG1 may be associated with NPC cell migration and metastasis.[81]

This approach provides a comprehensive view for understanding the complex mechanisms of SM and underscores the importance of computational biology tools in modern drug development.[82,83] Unlike conventional drug screening heavily reliant on empirical methods, this study predicts and validates SM's target effects through systematic network analysis, enhancing understanding its anti-NPC effects. This strategy not only expedites the discovery of drug targets but also boosts the scientific rigor and accuracy of research.[84–86] A recent study utilized network pharmacology to predict the effects of solamargine on lung adenocarcinoma and experimentally validated its impact on immune evasion via signaling pathways.[87] The experiments included colony formation, EDU staining, wound healing, Transwell assays, Hoechst staining, flow cytometry, as well as molecular signaling analysis through WB and RT-qPCR. While network pharmacology can predict drug-disease interaction targets, these predictions must be experimentally validated to confirm their efficacy. Future studies may provide further experimental evidence to support or refute these predictions.

Given the capabilities shown by SM in this study to inhibit NPC cell invasion and migration, as well as its inhibitory effect on angiogenesis, SM holds the potential to become a significant drug in NPC therapy. Particularly in preclinical models, if further confirmation of these effects can be achieved, they could usher in a new paradigm shift in NPC treatment strategies.[88] Considering the constraints of current NPC treatments, such as side effects and individual variations in treatment outcomes, the comprehensive regulatory mechanism of SM offers the potential for synergistic therapeutic effects, especially when combined with existing therapies, potentially demonstrating synergistic or additive effects.[89–91]

SM effectively inhibits NPC cell invasion and migration by regulating EMT and suppressing angiogenesis, enhancing our understanding of its anticancer mechanism and providing a scientific basis for clinical application. However, this study has limitations, primarily relying on in vitro experiments, and further validation through animal studies and clinical trials is needed. SM has been shown to inhibit human NPC cell growth[34] and suppress HBV by binding to myeloid zinc finger 1 (MZF1).[92] While the EBV-positive C666-1 cell line was used, whether SM induces or inhibits EBV reactivation remains unclear, which warrants further investigation. Additionally, the safety and potential side effects of SM need further evaluation. Previous studies indicate that SM inhibits tumor growth in lung adenocarcinoma and melanoma without significant toxicity (PMID: 38552432, 34,612,163). However, if SM exhibits strong cytotoxicity toward HUVEC cells, concerns about its clinical safety may arise. Further studies are required to assess its impact on normal endothelial cells and explore potential solutions such as dose adjustments or more selective analogs.

Conclusion

The study demonstrates that SM effectively inhibits NPC cell invasion and migration by regulating EMT markers and suppressing angiogenesis. Key mechanisms include the downregulation of EMT-related proteins such as Vimentin and Snail, suppression of the VEGF signaling pathway, and upregulation of miR-203a-3p. These findings highlight the therapeutic potential of SM in targeting multiple pathways involved in NPC progression and angiogenesis (Figure 8). SM emerges as a promising candidate for developing novel anti-cancer and anti-angiogenic therapies, warranting further investigation for its clinical application.

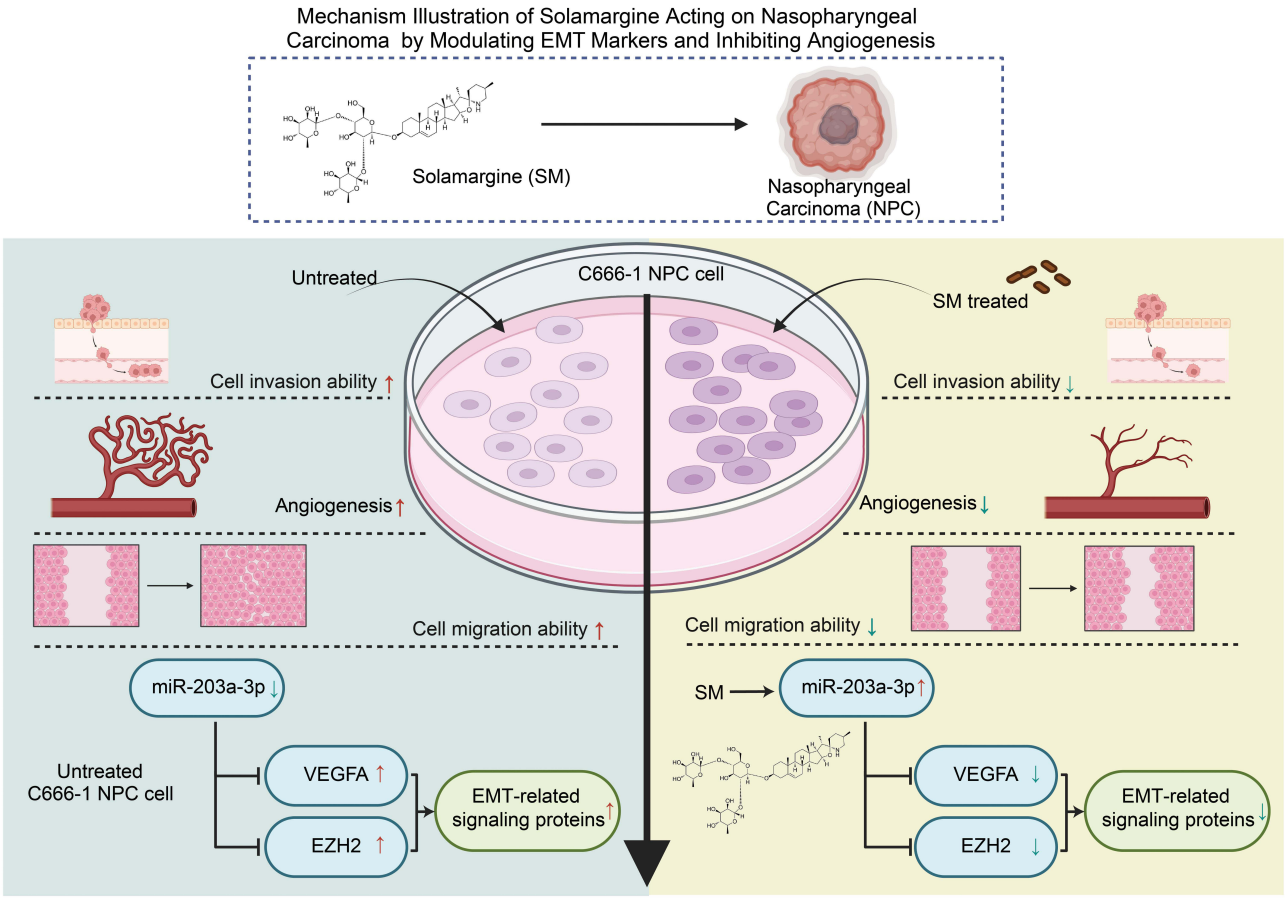

Figure 8 Mechanistic Schematic of Solorazin's Action on Nasopharyngeal Carcinoma through Modulation of EMT Markers and Inhibition of Angiogenesis.

Data Sharing Statement

All data can be provided as needed.

Ethical Approval

The cell lines used in this study were obtained from Sun Yat-sen Memorial Hospital, Guangzhou, Guangdong, China. All experimental protocols were approved by the institutional ethics committee and comply with the relevant ethical guidelines and regulations.

Author Contributions

All authors made a significant contribution to the work reported, whether that is in the conception, study design, execution, acquisition of data, analysis and interpretation, or in all these areas; took part in drafting, revising or critically reviewing the article; gave final approval of the version to be published; have agreed on the journal to which the article has been submitted; and agree to be accountable for all aspects of the work.

Funding

The current work funded by the Natural Science Foundation of Hunan Province of China (2024JJ6286), Natural Science Foundation of Changsha of Hunan Province (kq2403131), National Natural Science Foundation of China (82374462), Research Project of Hunan Provincial Administration of Tranditional Chinese Medicine (B2024031) and Health Research Project of Hunan Provincial Health Commission (W20243256).

Disclosure

The authors declare no conflicts of interest in this work.

References

1. Tang L, Chen Y, Chen C, et al. The Chinese society of clinical oncology (CSCO) clinical guidelines for the diagnosis and treatment of nasopharyngeal carcinoma. *Cancer Commun*. 2021;41(11):1195–1227. doi:10.1002/cac2.12218
2. Zhang Y, Rumgay H, Li M, Cao S, Chen W. Nasopharyngeal cancer incidence and mortality in 185 countries in 2020 and the projected burden in 2040: population-based global epidemiological profiling. *JMIR Public Health Surveill*. 2023;9:e49968. doi:10.2196/49968
3. Siak PY, Heng WS, Teoh SSH, Lwin YY, Cheah SC. Precision medicine in nasopharyngeal carcinoma: comprehensive review of past, present, and future prospect. *J Transl Med*. 2023;21(1). doi:10.1186/s12967-023-04673-8
4. Campion NJ, Ally M, Jank BJ, Ahmed J, Alusi G. The molecular march of primary and recurrent nasopharyngeal carcinoma. *Oncogene*. 2021;40 (10):1757–1774. doi:10.1038/s41388-020-01631-2
5. Tang L, Xu M, Zhu H, Peng Y. MiR-299-3p inhibits nasopharyngeal carcinoma cell proliferation and migration by targeting MMP-2. *J Oncol*. 2022;2022:1–7. doi:10.1155/2022/2322565
6. Chang ET, Ye W, Zeng YX, Adami HO. The evolving epidemiology of nasopharyngeal carcinoma. *Cancer Epidemiol Biomarkers Prev*. 2021;30 (6):1035–1047. doi:10.1158/1055-9965.epi-20-1702
7. Su ZY, Siak PY, Leong CO, Cheah SC. The role of Epstein–Barr virus in nasopharyngeal carcinoma. *Front Microbiol*. 2023;14. doi:10.3389/fmicb.2023.1116143
8. Peng X, Zhou Y, Tao Y, Liu S. Nasopharyngeal carcinoma: the role of the EGFR in Epstein–Barr virus infection. *Pathogens*. 2021;10(9):1113. doi:10.3390/pathogens10091113
9. Qin LT, Huang SW, Huang ZG, et al. Clinical value and potential mechanisms of BUB1B up-regulation in nasopharyngeal carcinoma. *BMC Med Genomics*. 2022;15(1). doi:10.1186/s12920-022-01412-8
10. Wang F, Li X, Li C. Mitochondrial non-coding RNA in nasopharyngeal carcinoma: clinical diagnosis and functional analysis. *Front Genet*. 2023;14. doi:10.3389/fgene.2023.1162332
11. Wang Z, Fang M, Zhang J, et al. Radiomics and deep learning in nasopharyngeal carcinoma: a review. *IEEE Rev Biomed Eng*. 2024;17:118–135. doi:10.1109/rbme.2023.3269776
12. Akf L, Dawson CW, Lung HL, Wong KL, Young LS. The role of EBV-Encoded LMP1 in the NPC tumor microenvironment: from function to therapy. *Front Oncol*. 2021;11. doi:10.3389/fonc.2021.640207
13. Sun Q, Wang Y, Ji H, et al. Lenvatinib for effectively treating antiangiogenic drug-resistant nasopharyngeal carcinoma. *Cell Death Dis*. 2022;13(8). doi:10.1038/s41419-022-05171-3
14. Liu Y, Wen J, Huang W. Exosomes in nasopharyngeal carcinoma. *Clin Chim Acta*. 2021;523:355–364. doi:10.1016/j.cca.2021.10.013
15. Yuan L, Jia GD, Lv XF, et al. Camrelizumab combined with apatinib in patients with first-line platinum-resistant or PD-1 inhibitor resistant recurrent/metastatic nasopharyngeal carcinoma: a single-arm, Phase 2 trial. *Nat Commun*. 2023;14(1). doi:10.1038/s41467-023-40402-x
16. Tang Y, He X. Long non-coding RNAs in nasopharyngeal carcinoma: biological functions and clinical applications. *mol Cell Biochem*. 2021;476 (9):3537–3550. doi:10.1007/s11010-021-04176-4
17. Li W, Duan X, Chen X, et al. Immunotherapeutic approaches in EBV-associated nasopharyngeal carcinoma. *Front Immunol*. 2023:13. doi:10.3389/fimmu.2022.1079515
18. Tang LL, Guo R, Zhang N, et al. Effect of radiotherapy alone vs radiotherapy with concurrent chemoradiotherapy on survival without disease relapse in patients with low-risk nasopharyngeal carcinoma. *JAMA*. 2022;328(8):728. doi:10.1001/jama.2022.13997
19. Mai HQ, Chen QY, Chen D, et al. Toripalimab plus chemotherapy for recurrent or metastatic nasopharyngeal carcinoma. *JAMA*. 2023;330 (20):1961. doi:10.1001/jama.2023.20181
20. Li JY, Zhao Y, Gong S, et al. TRIM21 inhibits irradiation-induced mitochondrial DNA release and impairs antitumour immunity in nasopharyngeal carcinoma tumour models. *Nat Commun*. 2023;14(1). doi:10.1038/s41467-023-36523-y
21. Huang H, Yao Y, Deng X, et al. Immunotherapy for nasopharyngeal carcinoma: current status and prospects. *Int J Oncol*. 2023;63(2). doi:10.3892/ijo.2023.5545
22. Weng H, Bejjanki NK, Zhang J, et al. TAT peptide-modified cisplatin-loaded iron oxide nanoparticles for reversing cisplatin-resistant nasopharyngeal carcinoma. *Biochem Biophys Res Commun*. 2019;511(3):597–603. doi:10.1016/j.bbrc.2019.02.117
23. Lyu M, Yi X, Huang Z, et al. A transcriptomic analysis based on aberrant methylation levels revealed potential novel therapeutic targets for nasopharyngeal carcinoma. *Ann Transl Med*. 2022;10(2):47. doi:10.21037/atm-21-6628
24. Liu ZL, Chen HH, Zheng LL, Sun LP, Shi L. Angiogenic signaling pathways and anti-angiogenic therapy for cancer. *Sig Transduct Target Ther*. 2023;8(1). doi:10.1038/s41392-023-01460-1
25. Lopes-Coelho F, Martins F, Pereira SA, Serpa J. Anti-angiogenic therapy: current challenges and future perspectives. *IJMS*. 2021;22(7):3765. doi:10.3390/ijms22073765
26. Chryplewicz A, Scotton J, Tichet M, et al. Cancer cell autophagy, reprogrammed macrophages, and remodeled vasculature in glioblastoma triggers tumor immunity. *Cancer Cell*. 2022;40(10):1111–1127.e9. doi:10.1016/j.ccell.2022.08.014
27. Tang Q, Li X, Chen Y, et al. Solamargine inhibits the growth of hepatocellular carcinoma and enhances the anticancer effect of sorafenib by regulating HOTTIP-TUG1/miR-4726-5p/MUC1 pathway. *Mol Carcinog*. 2022;61(4):417–432. doi:10.1002/mc.23389
28. Zhao F, Feng G, Zhu J, et al. 3-Methyladenine-enhanced susceptibility to sorafenib in hepatocellular carcinoma cells by inhibiting autophagy. *Anti-Cancer Drugs*. 2021;32(4):386–393. doi:10.1097/cad.0000000000001032
29. Wang CJ, Guo X, Zhai RQ, et al. Discovery of penipanoid C-inspired 2-(3,4,5-trimethoxybenzoyl)quinazolin-4(3H)-one derivatives as potential anticancer agents by inhibiting cell proliferation and inducing apoptosis in hepatocellular carcinoma cells. *Eur J Med Chem*. 2021;224:113671. doi:10.1016/j.ejmech.2021.113671
30. Zhang Z, Zeng X, Wu Y, Liu Y, Zhang X, Song Z. Cuproptosis-related risk score predicts prognosis and characterizes the tumor microenvironment in hepatocellular carcinoma. *Front Immunol*. 2022;13. doi:10.3389/fimmu.2022.925618

31. Li Z, Liao X, Hu Y, et al. SLC27A4-mediated selective uptake of mono-unsaturated fatty acids promotes ferroptosis defense in hepatocellular carcinoma. *Free Radic Biol Med*. 2023;201:41–54. doi:10.1016/j.freeradbiomed.2023.03.013
32. Shi Z, Li Z, Jin B, et al. Loss of LncRNA DUXAP8 synergistically enhanced sorafenib induced ferroptosis in hepatocellular carcinoma via SLC7A11 de-palmitoylation. *Clin Transl Med*. 2023;13(6). doi:10.1002/ctm2.1300
33. Ring SS, Cupovic J, Onder L, et al. Viral vector-mediated reprogramming of the fibroblastic tumor stroma sustains curative melanoma treatment. *Nat Commun*. 2021;12(1). doi:10.1038/s41467-021-25057-w
34. Wu J, Tang X, Ma C, Shi Y, Wu W, Hann SS. The regulation and interaction of colon cancer-associated transcript-1 and miR7-5p contribute to the inhibition of SP1 expression by solamargine in human nasopharyngeal carcinoma cells. *Phytother Res*. 2019;34(1):201–213. doi:10.1002/ptr.6555
35. Liu HY, Zhang YY, Zhu BL, et al. MiR-203a-3p regulates the biological behaviors of ovarian cancer cells through mediating the Akt/GSK-3β/Snail signaling pathway by targeting ATM. *J Ovarian Res*. 2019;12(1). doi:10.1186/s13048-019-0532-2
36. Han N, Xu H, Yu N, Wu Y, Yu L. MiR-203a-3p inhibits retinal angiogenesis and alleviates proliferative diabetic retinopathy in oxygen-induced retinopathy (OIR) rat model via targeting VEGFA and HIF-1α. *Clin Exp Pharma Physio*. 2019;47(1):85–94. doi:10.1111/1440-1681.13163
37. Yu L, Fu J, Yu N, Wu Y, Han N. Long noncoding RNA MALAT1 participates in the pathological angiogenesis of diabetic retinopathy in an oxygen-induced retinopathy mouse model by sponging miR-203a-3p. *Can J Physiol Pharmacol*. 2020;98(4):219–227. doi:10.1139/cjpp-2019-0489
38. Hu-Lowe DD, Zou HY, Grazzini ML, et al. Nonclinical antiangiogenesis and antitumor activities of axitinib (AG-013736), an oral, potent, and selective inhibitor of vascular endothelial growth factor receptor tyrosine kinases 1, 2, 3. *Clin Cancer Res*. 2008;14(22):7272–7283. doi:10.1158/1078-0432.ccr-08-0652
39. Jiang H, Liao J, Wang L, Jin C, Mo J, Xiang S. The multikinase inhibitor axitinib in the treatment of advanced hepatocellular carcinoma: the current clinical applications and the molecular mechanisms. *Front Immunol*. 2023;14. doi:10.3389/fimmu.2023.1163967
40. Download full text. doi:10.23812/20-724-L.
41. Wang CH, Lo CY, Huang HY, et al. Oxygen desaturation is associated with fibrocyte activation via epidermal growth factor receptor/hypoxia-inducible factor-1α axis in chronic obstructive pulmonary disease. *Front Immunol*. 2022:13. doi:10.3389/fimmu.2022.852713
42. Ye Y, Chen A, Li L, et al. Repression of the antiporter SLC7A11/glutathione/glutathione peroxidase 4 axis drives ferroptosis of vascular smooth muscle cells to facilitate vascular calcification. *Kidney Int*. 2022;102(6):1259–1275. doi:10.1016/j.kint.2022.07.034
43. Tang G, Li S, Zhang C, Chen H, Wang N, Feng Y. Clinical efficacies, underlying mechanisms and molecular targets of Chinese medicines for diabetic nephropathy treatment and management. *Acta Pharmaceutica Sinica B*. 2021;11(9):2749–2767. doi:10.1016/j.apsb.2020.12.020
44. Bai X, Zhao G, Chen Q, et al. Inhaled siRNA nanoparticles targeting IL11 inhibit lung fibrosis and improve pulmonary function post-bleomycin challenge. *Sci Adv*. 2022;8(25). doi:10.1126/sciadv.abn7162
45. Zhang J, Wang H, Chen H, et al. ATF3 -activated accelerating effect of LINC00941/lncIAPF on fibroblast-to-myofibroblast differentiation by blocking autophagy depending on ELAVL1/HuR in pulmonary fibrosis. *Autophagy*. 2022;18(11):2636–2655. doi:10.1080/15548627.2022.2046448
46. Burunova VV, Gisina AM, Yarygina NK, Sukhinich KK, Makiyan ZN, Yarygin KN. Isolation of a population of cells co-expressing markers of embryonic stem cells and mesenchymal stem cells from the rudimentary uterine horn of a patient with uterine aplasia. *Bull Exp Biol Med*. 2023;174(4):549–555. doi:10.1007/s10517-023-05746-w
47. Lee OZJ, Omar N, Tay JK, Lee VKM. A clinicopathology review and update of Epstein–Barr virus-associated mesenchymal tumors. *Cancers*. 2023;15(23):5563. doi:10.3390/cancers15235563
48. Wang J, Luo S, Li Y, Zheng H. Nasopharyngeal papillary adenocarcinoma harboring a fusion of ROS1 with GOPC. *Medicine*. 2021;100(3):e24377. doi:10.1097/md.0000000000024377
49. Xiao P, Gu J, Xu W, et al. RTN4/Nogo-A-S1PR2 negatively regulates angiogenesis and secondary neural repair through enhancing vascular autophagy in the thalamus after cerebral cortical infarction. *Autophagy*. 2022;18(11):2711–2730. doi:10.1080/15548627.2022.2047344
50. Yao H, Li J, Liu Z, et al. Ablation of endothelial Atg7 inhibits ischemia-induced angiogenesis by upregulating Stat1 that suppresses Hif1a expression. *Autophagy*. 2022;19(5):1491–1511. doi:10.1080/15548627.2022.2139920
51. Yang H, Song L, Sun B, et al. Modulation of macrophages by a paeoniflorin-loaded hyaluronic acid-based hydrogel promotes diabetic wound healing. *Mater Today Bio*. 2021;12:100139. doi:10.1016/j.mtbio.2021.100139
52. Neves KB, Alves-Lopes R, Montezano AC, Touyz RM. Role of PARP and TRPM2 in VEGF inhibitor-induced vascular dysfunction. *JAHA*. 2023;12(4). doi:10.1161/jaha.122.027769
53. Ma J, Li Y, Yang X, et al. Signaling pathways in vascular function and hypertension: molecular mechanisms and therapeutic interventions. *Sig Transduct Target Ther*. 2023;8(1). doi:10.1038/s41392-023-01430-7
54. Cao G, Xuan X, Hu J, Zhang R, Jin H, Dong H. How vascular smooth muscle cell phenotype switching contributes to vascular disease. *Cell Commun Signal*. 2022;20(1). doi:10.1186/s12964-022-00993-2
55. Lin J, Wang Q, Zhou S, Xu S, Yao K. Tetramethylpyrazine: a review on its mechanisms and functions. *Biomed Pharmacother*. 2022;150:113005. doi:10.1016/j.biopha.2022.113005
56. Lu Z, Huang M, Lin H, Wang G, Li H. Network pharmacology and molecular docking approach to elucidate the mechanisms of Liuwei Dihuang pill in diabetic osteoporosis. *J Orthop Surg Res*. 2022;17(1). doi:10.1186/s13018-022-03194-2
57. Farzaneh Behelgardi M, Gholami Shahvir Z, Asghari SM. Apoptosis induction in human lung and colon cancer cells via impeding VEGF signaling pathways. *Mol Biol Rep*. 2022;49(5):3637–3647. doi:10.1007/s11033-022-07203-9
58. Wong SWK, Tey SK, Mao X, et al. Small extracellular vesicle-derived vWF induces a positive feedback loop between tumor and endothelial cells to promote angiogenesis and metastasis in hepatocellular carcinoma. *Adv Sci*. 2023;10(26). doi:10.1002/advs.202302677
59. Critchley WR, Fearnley GWF, Abdul-Zani I, et al. Monitoring VEGF-stimulated calcium ion flux in endothelial cells. *Methods mol Biol*. 2022:113–124. doi:10.1007/978-1-0716-2217-9_7
60. Johnson RM, Qu X, Lin CF, et al. ARID1A mutations confer intrinsic and acquired resistance to cetuximab treatment in colorectal cancer. *Nat Commun*. 2022;13(1). doi:10.1038/s41467-022-33172-5
61. Dong X, Lei Y, Yu Z, et al. Exosome-mediated delivery of an anti-angiogenic peptide inhibits pathological retinal angiogenesis. *Theranostics*. 2021;11(11):5107–5126. doi:10.7150/thno.54755
62. Adachi Y, Kamiyama H, Ichikawa K, et al. Inhibition of FGFR reactivates IFNγ signaling in tumor cells to enhance the combined antitumor activity of lenvatinib with anti-PD-1 antibodies. *Cancer Res*. 2021;82(2):292–306. doi:10.1158/0008-5472.can-20-2426

63. Zhou W, Liu K, Zeng L, et al. Targeting VEGF-A/VEGFR2 Y949 signaling-mediated vascular permeability alleviates hypoxic pulmonary hypertension. *Circulation*. 2022;146(24):1855–1881. doi:10.1161/circulationaha.122.061900
64. Koide T, Mandai S, Kitaoka R, et al. circulating extracellular vesicle-propagated microRNA signature as a vascular calcification factor in chronic kidney disease. *Circul Res*. 2023;132(4):415–431. doi:10.1161/circresaha.122.321939
65. Worssam MD, Jørgensen HF. Mechanisms of vascular smooth muscle cell investment and phenotypic diversification in vascular diseases. *Biochem Soc Trans*. 2021;49(5):2101–2111. doi:10.1042/bst20210138
66. Li J, Liao R, Zhang S, et al. Promising remedies for cardiovascular disease: natural polyphenol ellagic acid and its metabolite urolithins. *Phytomedicine*. 2023;116:154867. doi:10.1016/j.phymed.2023.154867
67. Yang P, Zhang D, Zhou F, et al. miR-203a-3p-DNMT3B feedback loop facilitates non-small cell lung cancer progression. *Human Cell*. 2022;35(4):1219–1233. doi:10.1007/s13577-022-00728-y
68. Miao R, Yao Z, Hu B, et al. A novel long non-coding RNA XLOC_004787, is associated with migration and promotes cancer cell proliferation by downregulating mir-203a-3p in gastric cancer. *BMC Gastroenterol*. 2023;23(1). doi:10.1186/s12876-023-02912-2
69. van Nijnatten J, Brandsma CA, Steiling K, et al. High miR203a-3p and miR-375 expression in the airways of smokers with and without COPD. *Sci Rep*. 2022;12(1). doi:10.1038/s41598-022-09093-0
70. Deng W, Wang X, Chen L, et al. Proteomic and miRNA profiles of exosomes derived from myometrial tissue in laboring women. *IJMS*. 2022;23(20):12343. doi:10.3390/ijms232012343
71. Zhao H, Chang A, Ling J, Zhou W, Ye H, Zhuo X. Construction and analysis of miRNA-mRNA regulatory networks in the radioresistance of nasopharyngeal carcinoma. *3 Biotech*. 2020;10(12). doi:10.1007/s13205-020-02504-x
72. Karar J, Maity A. PI3K/AKT/mTOR pathway in angiogenesis. *Front Mol Neurosci*. 2011;4:4. doi:10.3389/fnmol.2011.00051
73. Yamamoto N, Ryoo BY, Keam B, et al. A Phase 1 study of oral ASP5878, a selective small-molecule inhibitor of fibroblast growth factor receptors 1–4, as a single dose and multiple doses in patients with solid malignancies. *Invest New Drugs*. 2019;38(2):445–456. doi:10.1007/s10637-019-00780-w
74. Azoitei N, Becher A, Steinestel K, et al. PKM2 promotes tumor angiogenesis by regulating HIF-1α through NF-κB activation. *Mol Cancer*. 2016;15(1). doi:10.1186/s12943-015-0490-2
75. Garg DK, Tomar R, Dhoke RR, Srivastava A, Kundu B. Domains of Pyrococcus furiosus l-asparaginase fold sequentially and assemble through strong intersubunit associative forces. *Extremophiles*. 2015;19(3):681–691. doi:10.1007/s00792-015-0748-z
76. Cho I, Jia ZJ, Arnold FH. Retraction. *Science*. 2020;367(6474):155. doi:10.1126/science.aba6100
77. Zhang X, Wang Y, Li Y, Liu Z, Sun T, Sun X. Measurement of the inner diameter of monocapillary with confocal x-ray scattering technology based on capillary x-ray optics. *Appl Opt*. 2019;58(5):1291. doi:10.1364/ao.58.001291
78. Brito R, Specht A, Gonçalves GL, et al. *Spodoptera marima*: a new synonym of Spodoptera *ornithogalli* (Lepidoptera: Noctuidae), with notes on adult morphology, host plant use and genetic variation along its geographic range. *Neotrop Entomol*. 2018;48(3):433–448. doi:10.1007/s13744-018-0654-z
79. Lei G, Cao N, McPherson BJ, Liao Q, Chen W. A novel analytical model for pore volume compressibility of fractal porous media. *Sci Rep*. 2019;9(1). doi:10.1038/s41598-019-51091-2
80. Xie W, Huang G, Cui B, et al. Characteristics and performance evaluation of QZSS onboard satellite clocks. *Sensors*. 2019;19(23):5147. doi:10.3390/s19235147
81. Dangi A, Agrawal S, Datta GR, Srinivasan V, Kothapalli SR. Towards a low-cost and portable photoacoustic microscope for point-of-care and wearable applications. *IEEE Sensors J*. 2020;20(13):6881–6888. doi:10.1109/jsen.2019.2935684
82. Piya D, Nolan N, Moore ML, et al. Systematic and scalable genome-wide essentiality mapping to identify nonessential genes in phages. *PLoS Biol*. 2023;21(12):e3002416. doi:10.1371/journal.pbio.3002416
83. Block LJ, Wong ST, Handfield S, Hart R, Currie LM. Comparison of terminology mapping methods for nursing wound care knowledge representation. *Int J Med Inform*. 2021;153:104539. doi:10.1016/j.ijmedinf.2021.104539
84. Gupta D, Zickler AM, El Andaloussi S. Dosing extracellular vesicles. *Adv Drug Delivery Rev*. 2021;178:113961. doi:10.1016/j.addr.2021.113961
85. Wu D, Chen Q, Chen X, Han F, Chen Z, Wang Y. The blood–brain barrier: structure, regulation and drug delivery. *Sig Transduct Target Ther*. 2023;8(1). doi:10.1038/s41392-023-01481-w
86. Zhao L, Zhang H, Li N, et al. Network pharmacology, a promising approach to reveal the pharmacology mechanism of Chinese medicine formula. *J Ethnopharmacol*. 2023;309:116306. doi:10.1016/j.jep.2023.116306
87. Liu Q, Xu M, Qiu M, et al. Solamargine improves the therapeutic efficacy of anti-PD-L1 in lung adenocarcinoma by inhibiting STAT1 activation. *Phytomedicine*. 2024;128:155538. doi:10.1016/j.phymed.2024.155538
88. Morar-Mitrica S, Pohl T, Theisen D, et al. An intra-company analysis of inherent particles in biologicals shapes the protein particle mitigation strategy across development stages. *J Pharmaceut Sci*. 2023;112(5):1476–1484. doi:10.1016/j.xphs.2023.01.023
89. McDonald EG, Aggrey G, Aslan AT, et al. Guidelines for diagnosis and management of infective endocarditis in adults. *JAMA Network Open*. 2023;6(7):e2326366. doi:10.1001/jamanetworkopen.2023.26366
90. Robichaud S, Fairman G, Vijithakumar V, et al. Identification of novel lipid droplet factors that regulate lipophagy and cholesterol efflux in macrophage foam cells. *Autophagy*. 2021;17(11):3671–3689. doi:10.1080/15548627.2021.1886839
91. Xiong A, Zhang J, Chen Y, Zhang Y, Yang F. Integrated single-cell transcriptomic analyses reveal that GPNMB-high macrophages promote PN-MES transition and impede T cell activation in GBM. *eBioMedicine*. 2022;83:104239. doi:10.1016/j.ebiom.2022.104239
92. Chen W, Zhao X, Huang Y, et al. Solamargine acts as an antiviral by interacting to MZF1 and targeting the core promoter of the hepatitis B virus gene. *Aging*. 2024. doi:10.18632/aging.206047